Proceedings of the
American Control Conference
Seattle, Washington • June 1995

Vehicle Longitudinal Control Using an Adaptive Observer for Automated Highway Systems

Sei-Bum Choi*and J.K. Hedrick†

University of California
Berkeley, CA 94720

Abstract

This paper summarizes data fusion, controller design and experimental work done recently for the longitudinal control of a platoon of autonomous vehicles. This paper presents alternative sub-models of an engine and a transmission to achieve the goal of precise spacing control with smooth ride quality. Adaptive observers are developed to estimate the vehicle-to-vehicle spacing and the closing rate. The estimated values are used in a sliding mode based controller. The developed control strategies are implemented on test vehicles and four vehicle platoon control performed at low to highway speed profiles using throttle position control alone.

1 Introduction

Over the decades Intelligent Transportation Systems(ITS) have become a topic of interest for development as a safe and efficient means of travel on congested highways. The California Partners for Advanced Transit and Highways (California PATH) has been developing advanced vehicle control systems (AVCS) required for ITS. These systems attempt to control the lateral and longitudinal motions of all vehicles in a multi-vehicle platoon system, and this paper presents recent work on the longitudinal control of a platoon of autonomous vehicles.

There has been a lot of research conducted on longitudinal control of AVCS. Hedrick and Sheikholeslam have proposed controllers using a spacing control strategy, and Ioannou has proposed controllers using a headway control strategy [4][7][9]. Swaroop has studied string stability to eliminate collisions due to the amplifications of the spacing errors in the platoon [11]. However, most of the previous studies have been limited to analysis and simulation, and even the implementation of the control code on the test vehicle has not shown good results, since practical issues like sensing error, plant/model mismatch and time delay/lag were not considered enough [5]. In this paper, the vehicle model is based on Cho and Hedrick's engine model [1]. However, throttle body and torque converter sub-models are modified. Sliding mode control law is modified to get more safety margin of stability without increasing the control gain. Several distance estimation schemes are suggested and evaluated in a four-vehicle platoon control.

2 Vehicle Model for Longitudinal Control

This section gives a vehicle model for longitudinal speed control. The model is based on Cho and Hedrick's continuous engine model [1]. The sub-models considered are engine, intake manifold and torque converter. Other parts of the power train are assumed to be rigid and the tire mode and slip are not considered.

2.1 Engine

The continuous engine model is described by:

$$\dot{\omega}_e = \frac{1}{I_e}\left[T_{net}(\omega_e, m_a) - T_L\right] \tag{1}$$

where T_{net} is the net combustion torque (indicated torque − friction torque), T_L the external torque on the engine, I_e the equivalent rotational inertia of the vehicle on the engine, ω_e the engine speed and m_a the mass of air in the intake manifold. If each cylinder event is neglected and constant air-to-fuel ratio assumed, T_{net} is a function of only ω_e and m_a [2].

2.2 Intake Manifold

The assumptions in the modeling of the intake manifold are:

- the air in the intake manifold obeys the ideal gas law
- all properties (pressure and temperature) are uniform throughout the volume of the manifold
- the temperature of the air in the intake manifold is constant or changing very slowly
- the presence of fuel has no effect on the air flow
- the amount of E.G.R. is negligible

Neglecting the effects of individual intake strokes and the pulsation of the air, the continuity equation of the manifold volume is:

$$\dot{m}_a = \dot{m}_{ai}(\alpha, P_m/P_{atm}) - \dot{m}_{ao}(\omega_e, m_a) \tag{2}$$

$$P_m V_m = m_a R T_m \tag{3}$$

where $\dot{m}_{ai}$ means the air flow rate through the throttle body, $\dot{m}_{ao}$ the air flow rate into the cylinder, α the throttle angle, P_m the manifold air pressure, P_{atm} the atmospheric air pressure, V_m the manifold volume, R the ideal gas constant and T_m the manifold air temperature.

Assuming the throttle body air flow $\dot{m}_{ai}$ as one-dimensional isentropic compressible flow across an orifice, the variables α and P_m can be separated as [8]:

$$\dot{m}_{ai} = MAX\ TC(\alpha)\ PRI(P_m/P_{atm}) \tag{4}$$

where MAX is a constant dependent on the size of the throttle body, $TC(\alpha)$ the throttle characteristic which is the projected area the flow sees as a function of α, and PRI the pressure influence function which describes the choked flow rate as a function of the pressure drop across an orifice.

This one dimensional model is simple but has some error due

*California PATH, e-mail: choi@vehicle.berkeley.edu
†Mech. Eng. Dept, e-mail: khedrick@euler.berekely.edu

to the separation of the variables; the air flow is not exactly one dimensional and the shape of the opening area is not uniform. The error is not negligible depending upon the operation conditions, since the throttle command α can be expressed as:

$$\alpha = TC^{-1}\left[\frac{\dot{m}_{ai}}{MAX\,PRI}\right] \tag{5}$$

For example, both $\dot{m}_{ai}$ and PRI can be quite small and a tiny change of PRI makes a big difference on α the throttle command. Therefore, in this paper, a two-dimensional model given in equation (2) as $\dot{m}_{ai}(\alpha, P_m/P_{atm})$ is adopted.

2.3 Torque Converter

The torque converter consists of a pump attached to the engine and a turbine to the driving axle through the transmission. Neglecting the inertia of the transmission oil, the converter can be assumed to be a static element, but some phase lag/time delay was observed during the field test. [3].

On each side, the torque is related to the speed ratio ($\triangleq \omega_t/\omega_p$) as:

$$T_t = \left(\frac{\omega_t}{C_{tr}}\right)^2 \tag{6}$$

$$T_p = \left(\frac{\omega_p}{C_{pr}}\right)^2 \tag{7}$$

where (T_t, ω_t, C_{tr}) and (T_p, ω_p, C_{pr}) mean the torques, the speeds and the capacity factors of the turbine and the pump. Since the capacity factors are functions of the speed ratio, T_t, ω_t, T_p and ω_p are coupled to each other, and the change of one affects the other three.

3 Platoon Spacing Control Law

The objective of the platoon spacing control is to make the closed loop system (a string of vehicles) asymptotically stable to external disturbances and to keep the spacing to a preset constant. One way to satisfy this requirement is to have the maximum absolute spacing error of j-th vehicle less than or equal to that of the j-1st vehicle. Define the spacing error ϵ_j of the j-th vehicle to be:

$$\epsilon_j \triangleq x_{j-1} - x_j - L_j \tag{8}$$

$$\dot{\epsilon}_j \triangleq \dot{x}_{j-1} - \dot{x}_j \tag{9}$$

where L_j is the constant target distance between j-th vehicle and j-1st. Define:

$$\omega_o(t) \triangleq v_o(t) - v_o(0-) \tag{10}$$

where $v_o(t)$ is the velocity of the lead vehicle. Since the control input to keep the distance is the engine torque, the problem can be normalized as:

$$\ddot{x}_j = u_j \tag{11}$$

Assuming that the information from the preceding vehicle and the leading one is available, consider the following control law [4] [11]:

$$\begin{aligned} u_j &= k_p\,\epsilon_j + k_v\,\dot{\epsilon}_j + k_o\,a_o + k_a\,a_{j-1} \\ &- c_p\left[x_j(t) - x_o(t) + \sum_1^j L_i\right] \\ &- c_v\left[\dot{x}_j(t) - \dot{x}_o(t)\right] \quad , \quad j > 1 \end{aligned} \tag{12}$$

and

$$u_1 = (k_p + c_p)\,\epsilon_1 + (k_v + c_v)\,\dot{\epsilon}_1 + (k_a + k_o)\,a_o \tag{13}$$

where a_o is the acceleration of the lead vehicle, a_{j-1} the j-1st vehicle(j-th vehicle's predecessor) and x_o the position of the lead vehicle. If the lead vehicle position information is not available (i.e., $c_p = 0$), the transfer functions of the spacing error transmitted are given as:

$$\hat{g} \triangleq \frac{\hat{\epsilon}_1}{\hat{\omega}_o}(s) = -\frac{(k_a + k_o - 1)\,s}{s^2 + (k_v + c_v)\,s + k_p} \tag{14}$$

$$\hat{h} \triangleq \frac{\hat{\epsilon}_i}{\hat{\epsilon}_{i-1}}(s) = \frac{k_a\,s^2 + k_v\,s + k_p}{s^2 + (k_v + c_v)\,s + k_p} \tag{15}$$

For any positive k_v, c_v and k_p, the characteristic polynomials of $\hat{g}(s)$ and $\hat{h}(s)$ are Hurwitz, and if:

$$c_v > \sqrt{k_v^2 + 2\,k_p\,(1 - k_a)} - k_v \tag{16}$$

the string stability condition, i.e. $|\hat{h}(j\omega)| < 1$ for any ω, is satisfied [11].

4 Engine Control Laws

Since the control input u_j (j = 1, 2, 3....) is the desired acceleration of j-th vehicle, if the vehicle inertia, the wheel radius and the gear reduction ratio are given, the equivalent turbine torque T_t of the torque converter is obtained. If the clutch in the torque converter is engaged,

$$T_{net\_des} \triangleq T_{p\_des} = T_{t\_des} \tag{17}$$

where T_{net_des}, T_{p_des} and T_{t_des} are the desired torque of the engine, the pump and the turbine. Since T_{net} is a function of m_a and ω_e, for a given ω_e:

$$m_{a\_des} = m_{a\_des}(T_{net\_des},\, \omega_e) \tag{18}$$

Since m_{a_des} is not an explicit function of the control input α, define:

$$S_2 \triangleq m_a - m_{a\_des} \tag{19}$$

and, if S_2 satisfies:

$$\dot{S}_2 = -\lambda_2\,S_2 \quad , \quad \lambda_2 > 0 \tag{20}$$

then, S_2 goes to zero exponentially [2]. Substituting equation (2) into equation (20):

$$\begin{aligned} \dot{m}_{ai\_des}(\alpha_{des},\, P_m/P_{atm}) &= \dot{m}_{ao}(\omega_e,\, m_a) + \dot{m}_{a\_des} \\ &- \lambda_2\,(m_a - m_{a\_des}) \end{aligned} \tag{21}$$

or

$$\alpha_{des} = \alpha_{des}(\dot{m}_{ai\_des},\, P_m/P_{atm}) \tag{22}$$

where $\dot{m}_{ai\_des}$ is the desired air flow rate through the throttle body and α_{des} is the equivalent throttle angle. Here, $\dot{m}_{ao}$ is a function of ω_e and m_a, and using m_{a_des}(or P_{m_des}) instead of m_a(or P_m) makes the closed loop system more stable [2]. Due to the same reason that $\frac{\partial \dot{m}_{ai}}{\partial P_m}|_\alpha < 0$ for any P_m, P_{m_des} is used instead of P_m in obtaining α_{des}, i.e.:

$$\begin{aligned} \dot{m}_{ai\_des}(\alpha_{des},\, P_{m\_des}/P_{atm}) &= \dot{m}_{ao}(\omega_e,\, m_{a\_des}) + \dot{m}_{a\_des} \\ &- \lambda_2\,(m_a - m_{a\_des}) \end{aligned} \tag{23}$$

$$\alpha_{des} = \alpha_{des}(\dot{m}_{ai\_des},\, P_{m\_des}/P_{atm}) \tag{24}$$

If the clutch is not engaged, define T'_{net_des} as:

$$T'_{net\_des} \triangleq T_{t\_des} \tag{25}$$

and if the desired turbine torque T_{t_des} is given, C_{tr_des}, therefore ω_{e_des} (note that $\omega_{e\_des} = \omega_{p\_des}$), is obtained from equation (6). Define:

$$S_3 \triangleq \omega_e - \omega_{e\_des} \tag{26}$$

If

$$\dot{S}_3 = -\lambda_3 S_3 \ , \quad \lambda_3 > 0 \tag{27}$$

then ω_e converges to ω_{e_des} exponentially. Since

$$\dot{\omega}_e = \frac{1}{I_{eng}} [T_{net} - T_p] \tag{28}$$

where I_{eng} is the inertia of the engine and T_p the pump torque of the torque converter, combining equations (27) and (28):

$$T_{net\_des} = I_{eng} [\dot{\omega}_{e\_des} - \lambda_3 (\omega_e - \omega_{e\_des})] + T_p \tag{29}$$

and throttle command α_{des} can be obtained in the same procedure as in equations (18) - (24).

At the low gear states, the engine is not connected to the driving wheels mechanically, and there exists torque converter slip. Especially at a very low wheel speed, the slip is not negligibly small and the torque converter should be considered in the control, since the turbine torque is much bigger than the pump torque in that case and, if it is not considered, the control input becomes excessive. However, at a normal to high wheel speed, the slip is negligible.

5 Distance Observer

As figure 1 shows, the control laws developed in sections 3 and 4 work well in the case of single vehicle trajectory following. The remaining problem is how to get ϵ_j the vehicle-to-vehicle distance and $\dot{\epsilon}_j$ the closing rate. ϵ_j is measured using a distance sensor like a radar, but normally the measured signal is too noisy to be used directly in the control law. Since simple low pass filtering causes phase lag, a constant gain Kalman filter is considered:

$$\dot{\hat{\epsilon}} = e_{meas} + K (\epsilon_{meas} - \hat{\epsilon}) \tag{30}$$

where ϵ_{meas} and e_{meas} are the measured values of the spacing error and the closing rate, and $\hat{\epsilon}$ is the observed value of ϵ. If $\dot{\epsilon}$ can be measured exactly, a very smooth observation of ϵ is possible without any phase lag by choosing a small gain K. The steady state observation error of equation (30) is:

$$\tilde{\epsilon}|_{ss} \triangleq (\epsilon_{meas} - \hat{\epsilon})|_{ss} = \frac{|e_{meas}|}{K} \tag{31}$$

If K is big, the noise on ϵ_{meas} cannot be filtered out enough, and if K is small, the steady state observation error $\tilde{\epsilon}|_{ss}$ becomes very sensitive to the error on e_{meas}. In this study, e_{meas} is obtained from the wheel speed sensors and observed to have up to 5 % measurement error depending on the calculated effective wheel radius.

6 Adaptive Distance Observers

The only way to filter out the noise while minimizing the observation error is to get the closing rate exactly. Therefore, an adaptive observer is suggested as follows:

$$\dot{\hat{\epsilon}} = (e_{meas} + e_o) + K (\epsilon_{meas} - \hat{\epsilon}) \ , \quad K > 0 \tag{32}$$

If e_o can be updated to compensate for the error on e_{meas}, then a small gain K can be chosen while minimizing the steady state observation error. Let e_o be updated by:

$$\dot{e}_o = C (\dot{\epsilon}_{meas} - e_{meas} - e_o) \ , \quad C > 0 \tag{33}$$

Equations (32) and (33) can be written as:

$$\begin{bmatrix} \dot{\hat{\epsilon}} \\ \dot{e}_o \end{bmatrix} = \underbrace{\begin{bmatrix} -K & 1 \\ 0 & -C \end{bmatrix}}_{A} \begin{bmatrix} \hat{\epsilon} \\ e_o \end{bmatrix} + \begin{bmatrix} e_{meas} + K \epsilon_{meas} \\ C (\dot{\epsilon}_{meas} - e_{meas}) \end{bmatrix} \tag{34}$$

Since matrix A is Hurwitz and $C (\dot{\epsilon}_{meas} - e_{meas})$ is a constant or slowly varying, e_o converges to $(\dot{\epsilon}_{meas} - e_{meas})$ or $e_{meas} + e_o$ to $\dot{\epsilon}_{meas}$. Therefore, from equation (32):

$$\dot{\hat{\epsilon}} - \dot{\epsilon}_{meas} = K (\epsilon_{meas} - \hat{\epsilon}) \tag{35}$$

or

$$(\epsilon_{meas} - \hat{\epsilon}) \longrightarrow 0 \tag{36}$$

In the case that e_{meas} is obtained from the wheel speed sensors, the measurement error (=wheel radius measurement error × wheel rotating speed) is proportional to the wheel speed. Therefore, equations (32) and (33) can be modified as:

$$\dot{\hat{\epsilon}} = (e_{meas} + e_o v) + K (\epsilon_{meas} - \hat{\epsilon}) \ , \quad K > 0 \tag{37}$$

$$\dot{e}_o = C \left[\frac{(\dot{\epsilon}_{meas} - e_{meas})}{v} - e_o \right] \ , \quad C > 0 \tag{38}$$

where v is the vehicle velocity.

Even though ϵ and $\dot{\epsilon}$ are observed exactly, other errors on the engine modeling cause steady state error. One way to solve this problem is adding an integral term on the control law as:

$$u_j^* = u_j + k_i \int \epsilon_j(t)\, dt \tag{39}$$

Even though the steady state offset error can be reduced in this way, this makes the closed loop system less stable and causes more spacing error during quick maneuvers as the experimental results show in the next section.

7 Experimental Work

7.1 Test Setup

Experimental work on the vehicle longitudinal control is conducted using Lincoln Town Cars. Every vehicle is equipped with a 33 MHz 80486 IBM-PC compatible personal computer, an ultrasonic ranging system, a radar ranging system, a data communication system and a throttle actuator/controller. The interface to sensors and actuators is through National Instruments data acquisition boards. The data sampling and the control law run at 20 *msec* loop time under QNX real time operation system.

The ultrasonic ranging system and the radar ranging system are mounted in front of the radiator grill and they operate independently. Even though the ultrasonic system works very poorly at high vehicle speed, it is a good reference to evaluate other ranging systems at low vehicle speed to static.

The throttle is actuated by a stepper motor mounted on the throttle body and linked to the throttle plate. The motor has a maximum speed of 1000 *steps/sec* and 0.9 *deg/step* in a half-step mode, and is driven by the pulse generator/controller developed at California PATH.

The states of the vehicles are broadcast and received through PROXIM spread-spectrum radio transceivers and they are controlled by AT/Comm interface cards. The communication operation is performed at a rate of 121 *Kbits/sec* and 902 - 928 *MHz* band, which is approved by the Federal Communications Commission for unlicensed low power use. The radio

link is set to broadcast the velocity and acceleration of every vehicle. In the case of four-vehicle platooning, the loop time of the communication link is set to 50 *msec* for the limitation of the transceivers.

7.2 Platoon Control Test

This section presents the test results of several four-vehicle platoon controls performed on the High Occupant Vehicle (HOV) lanes of freeway I-15, San Diego, California, at 4 meter target distance.

Figure 1 shows a single vehicle trajectory following using the sliding mode engine control law developed in section 4. The trajectory was chosen to be able to follow by the throttle control alone. As the results show, a good tracking with a smooth throttle can be achieved. Therefore, the remaining problem is how to get or estimate the actual vehicle-to-vehicle distance and closing rate from the measured data for the multi-vehicle platooning.

Figures 2 and 3 show the behavior of the adaptive distance observers given in equations (32) and (33), and equations (37) and (38). Both of them filter out measurement noise very effectively, but the modified scheme is dominant during the transient operation of the vehicles (20 - 25 *sec*) and the adaptive parameter e_o stays more constant (see figure 4).

Figure 5 shows four-vehicle platoon control using the distance observer given in equation (30). As expected, large steady state errors are observed depending upon the velocity calibrations of the test vehicles and the observed distances do not converge to the measured. Even though the calibration errors are less than 5 %, the resulting offset errors are not negligibly small.

Figure 6 shows the same control using the adaptive distance observer given in equations (37) and (38), and the steady state error is significantly reduced compared to figure 5.

Figure 7 shows the control with the integral term fed back as in equation (39) in addition to the adaptive observer of equations (37) and (38). The steady state offset error is reduced, but this term causes more spacing errors at the moments of very fast maneuvers (130 - 170 *sec*, 190 - 210 *sec*).

8 Conclusions

The control laws, developed based on the nonlinear engine model and combined with the adaptive distance observers, showed very good tracking performances. The spacing perturbation error remained within $\pm$ 0.3 *meters* most of the time, but additional steady state offset error was found depending upon the operating condition. The throttle did not chatter much, so the ride quality, i.e. the vehicle acceleration, was quite smooth. The platoon string was observed to be stable. However, more spacing error was found during the quick transient maneuvers.

ACKNOWLEDGMENTS

The authors thank Pete Devlin and Leon Chen of the California PATH Program for their assistance throughout the test program.

References

[1] D. Cho and J.K. Hedrick, "Automotive Powertrain Modeling for Control", ASME Transactions on Dynamic System, Measurements and Control, Vol. 111, December, 1989.

[2] S.-B. Choi and J.K. Hedrick, "Design of a Robust Controller for Automotive Engines: Theory and Experiment", Ph.D. Thesis, U.C. Berkeley, August, 1993.

[3] S.-B. Choi, "Vehicle Longitudinal Control Test", PATH Working paper, U.C. Berkeley, Institute of Transportation Studies, UCB-ITS-D94-22, 1994.

[4] J.K. Hedrick, D.H. McMahon, V.K. Narendran and D. Swaroop, "Longitudinal Vehicle Controller Design for IVHS Systems", Proceedings of American Control Conference, pp 3107-3112, 1991.

[5] J.K. Hedrick, D.H. McMahon and D. Swaroop, "Vehicle Modeling and Control for Automated Highway Systems", PATH Report, U.C. Berkeley, Institute of Transportation Studies, UCB-ITS-PRP-93-24, 1993.

[6] J.K. Hedrick, etc., "Automated Highway System experiments in the PATH Program", Washington,D.C., Proceedings of the IVHS America, pp 131-146, 1992.

[7] P. Ioannou, C.C. Chien and J. Hauser, "Autonomous Intelligent Cruise Control", IVHS America, May 1992.

[8] J.J. Moskwa and J.K. Hedrick, "Modeling and Validation of Automotive Engines for Control Algorithm Development", ASME Winter Annual Meeting, Advanced Automotive Technologies, DSC-Vol. 13, 1989.

[9] S. Sheikholeslam, "Control of a Class of Interconnected Nonlinear Dynamical Systems", Ph.D. Dissertation, U.C. Berkeley, Dec. 1991.

[10] J.J.E. Slotine and W. Li, "Applied Nonlinear Control", Prentice Hall, 1991.

[11] D. Swaroop, C.D. Rizzuti and J.K. Hedrick, "Limitations of Alternative Platoon Control Strategies for IVHS", ASME Winter Annual Meeting, Transportation Systems, DSC-Vol. 54, 1994.

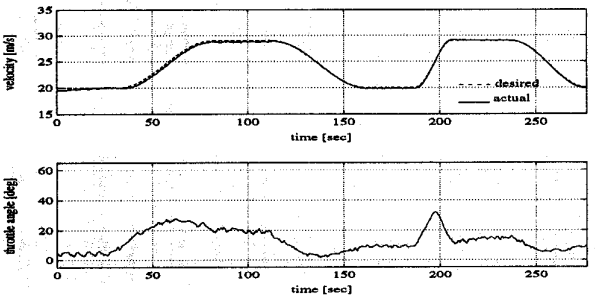

Figure 1: Single Vehicle Trajectory Following

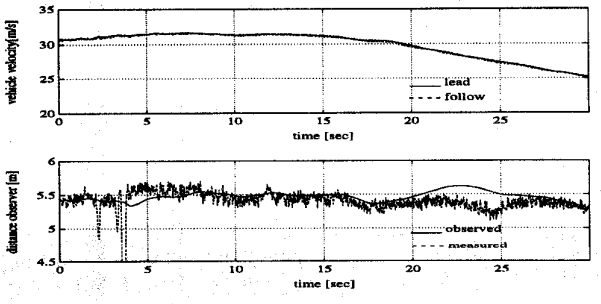

Figure 2: Adaptive Distance Observation

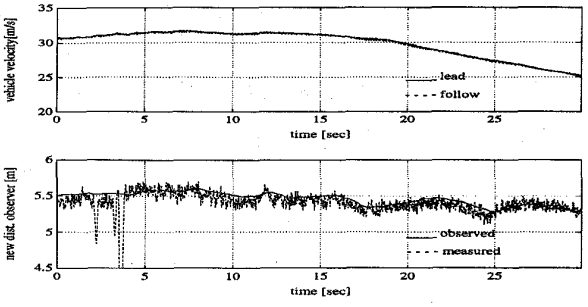

Figure 3: Modified Adaptive Distance Observation

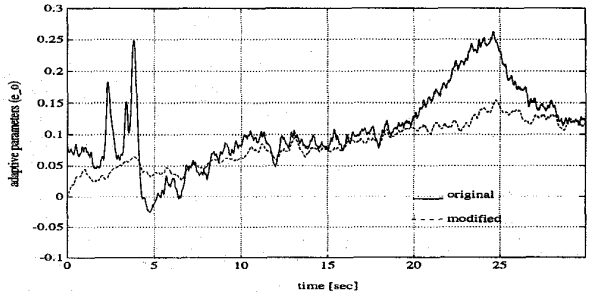

Figure 4: Adaptive Parameters of the Observers

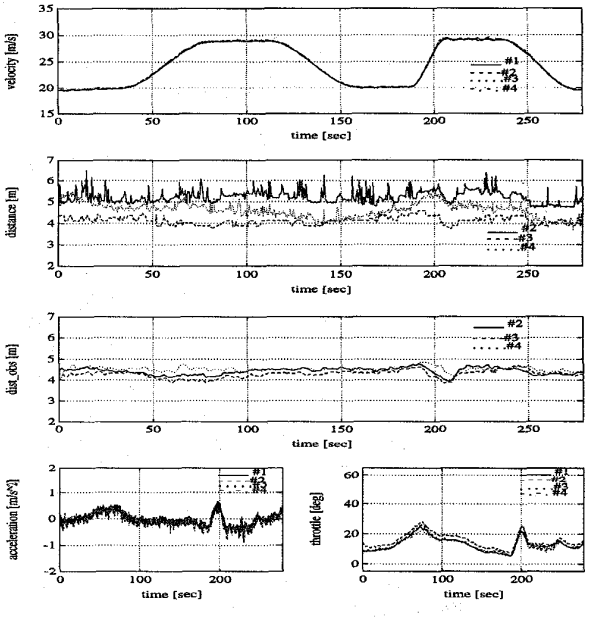

Figure 5: Four-Vehicle Platoon Control Using a Distance Observer

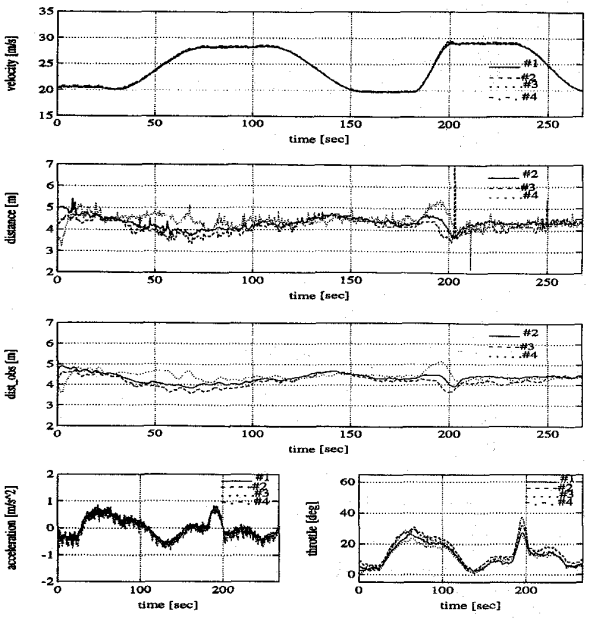

Figure 6: Four-Vehicle Platoon Control Using an Adaptive Distance Observer

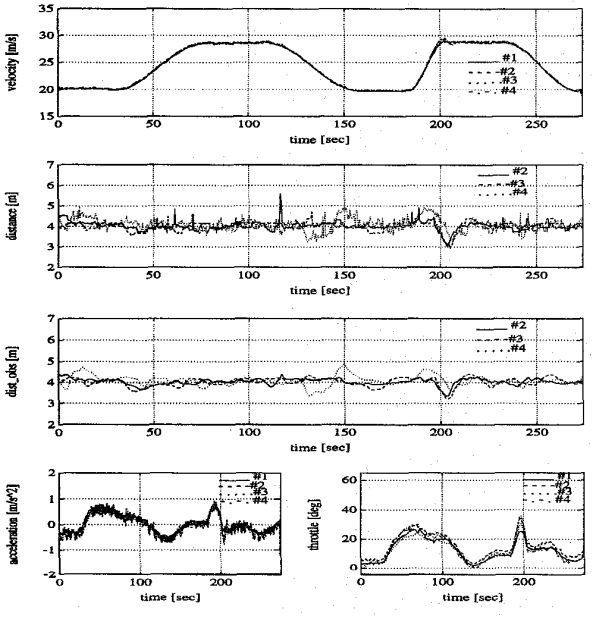

Figure 7: Four-Vehicle Platoon Control Using an Adaptive Distance Observer with the Integral of the Spacing Error Fed Back